Scattering and guiding characteristics of waveguides with two-dimensionally periodic walls of finite thickness

R. B. Hwang

Graduate Institute of Communication Engineering, National Chi Nan University, Puli, Nantou, Taiwan

S. T. Peng

Microelectronics and Information Systems Research Center, National Chiao-Tung University, Hsinchu, Taiwan

Received 26 November 2002; revised 27 May 2003; accepted 8 July 2003; published 23 October 2003.

[1] Electromagnetic wave propagation along waveguides having two-dimensionally (2-D) periodic walls with finite thickness is formulated here as an exact boundary-value problem. The dispersion relation of such a class of waveguide is systematically analyzed in terms of both phase and attenuation constants. In addition, the contour map of field components and Poynting vector are also demonstrated in this paper to verify the guiding characteristics of such a class of waveguides. In particular, the strong couplings between an incident plane wave and waveguide modes phase-matching condition are carefully examined and are employed to identify the existence of waveguide modes. *INDEX TERMS:* 0619 Electromagnetics: Electromagnetic theory; 0624 Electromagnetics: Guided waves; 0669 Electromagnetics: Scattering and diffraction; 0649 Electromagnetics: Optics; *KEYWORDS:* 2-D periodic structures, 1-D periodic structure, stop band, artificial crystal waveguide, photonic crystal waveguide, photonic band gap

Citation: Hwang, R. B., and S. T. Peng, Scattering and guiding characteristics of waveguides with two-dimensionally periodic walls of finite thickness, *Radio Sci.*, *38*(5), 1091, doi:10.1029/2002RS002847, 2003.

1. Introduction

[2] The development of artificial materials by constructing lattice structures has gained considerable attention in recent years; in particular, the stop-band phenomenon associated with lattice structures has found many applications. For example, an antenna substrate etched with two-dimensionally (2-D) periodic holes has been utilized to suppress the surface waves introduced by printed antenna [*Yang*, 1996; *Gauthier et al.*, 1997; *Papapolymerou et al.*, 1998; *Lubecke et al.*, 1998]. The 2-D periodic layers in conjunction with planar structures have been investigated for both optical and microwave applications; one example is a high impedance surface that will not support a surface wave in any direction [*Sievenpiper et al.*, 1999; *Yang et al.*, 1999]. A 2-D periodic impedance surface has been employed as a simplified model to study its scattering and guiding characteristics, especially for its stop-band behaviors in bound-wave and leaky-wave regions [*Hwang and Peng*, 1999a, 1999b]. A 2-D periodic array of dielectric rods in a uniform surrounding has been shown to exhibit many interesting phenomena, such as spontaneous emission and localization of electromagnetic energy. The large pixels (square rods of dielectric material) have been proved to be able to obtain a very large absolute band gap [*Shen et al.*, 2002]. In addition, they also provided a fast plane-wave expansion method to speed up the computation for the band structure. Specifically, the periodic arrays of dielectric materials were employed as a novel waveguide to mold the flow of electromagnetic energy or as a novel cavity to store the energy [*Mekis et al.*, 1999; *Maystre*, 1994; *Joannopoulos et al.*, 1995; *Noponen and Turunen*, 1994; *Vardaxoglou et al.*, 1993]. Although the phenomenon of waveguiding in such a class of structures has been demonstrated by means of numerical and experimental studies, the purpose of this work is to gain a clear physical picture of wave processes involved and to develop design rules for practical considerations.

[3] The basic concept of this class of applications can be traced back to the early work of *Larsen and Oliner* [1967], who had used one-dimensionally (1-D) periodic dielectric slabs to form waveguide walls that are operated in their stop-band or below-cutoff condition. In this paper, we extend the structure to the two-dimensional

0048-6604/03/2002RS002847

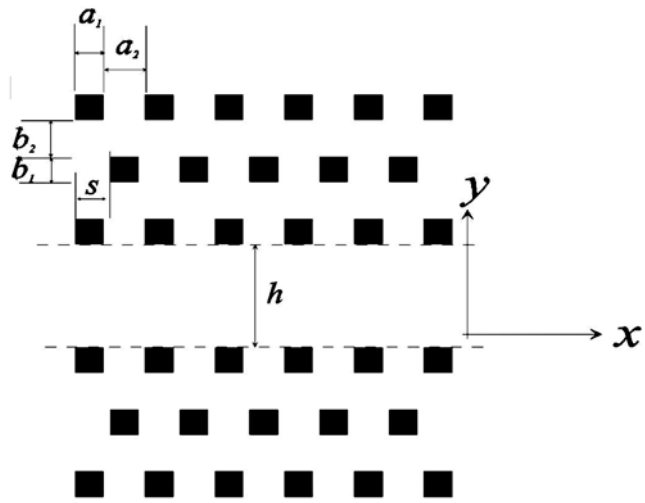

Figure 1. Structure configuration of waveguide with 2-D periodic walls of finite thickness.

case; that is, we replace the waveguide walls by finite stacks of 1-D periodic layers rather than uniform ones. For the purpose of comparison, the guiding characteristics of waveguides with uniform periodic dielectric layers are also investigated [*Hwang and Peng*, 2002].

[4] Specifically, the structure under consideration is a waveguide with 2-D periodic walls made of rectangular dielectric rods array immersed in a uniform surrounding, such as air. The 2-D periodic array is composed of a finite number of one-dimensionally periodic layers that are stacked with equal spacing between two neighboring ones. Each periodic layer is composed of an infinite number of rectangular dielectric rods of infinite length. In addition, we may displace every second row by a fractional part of the period to have any 2-D lattice pattern, so that the effect of the array pattern can be systematically investigated with ease. In this work, we shall employ the transverse resonance technique to obtain the dispersion relation; thus, the first step is to study the scattering characteristics of 2-D periodic dielectric rods array with finite thickness.

[5] The scattering characteristics of such a structure can be easily analyzed as a multilayer boundary-value problem. Here, we take the building block approach, such that the overall 2-D periodic structure can be regarded as a stack of unit cells, each consisting of a 1-D periodic layer in junction with a uniform one. By the rigorous method of mode matching, the input-output relation of a unit cell and the field distributions therein can be determined in a straightforward manner. It is noted that the present method offers a flexible approach to the analysis of 1-D periodic layer with arbitrary profile by making use of the staircase approximation to model it as a stack of cascaded 1-D periodic layers with different sizes of dielectric rods. In the absence of any incident wave, the existence of a non-trivial solution defines the condition of resonance in the transverse direction of the waveguide; in turn, this determines the dispersion relation of the waveguide.

[6] Based on the exact approach described above, we have carried out extensive numerical results to identify and explain the physical phenomena associated with the type of waveguides with 2-D periodic walls of finite thickness. Their dispersion characteristics are displayed in terms of both phase and attenuation constants. In particular, the contour plot for electric and magnetic field components and distribution of Poynting vector are used to gain a better understanding of the physical processes involved in the waveguiding in such a type of structures. Besides, the strong coupling between the incident plane wave and guided modes has also been studied in detail, including the mutual verification with the field and Poynting-vector distribution in the structure; these results establish consistently the distinctive characteristics of the waveguide with 2-D periodic walls of finite thickness from different viewpoints.

2. Statement of Problem

[7] Figure 1 shows a periodic structure with a finite number of unit cells, each consisting of a periodic layer in junction with a uniform one. While each periodic layer is composed of an infinite number of rectangular dielectric rods of infinite length, the structure can be viewed as an unbounded 2-D periodic medium, particularly when the number of the periodic layers in a stack is increased indefinitely. Therefore, we may infer the propagation characteristics of the 2-D periodic medium by the scat-

tering characteristics of a stack of sufficiently large number of 1-D periodic layers. With the coordinate system attached therein, the dielectric rods in each layer has the width a_1 and the distance between two neighboring rods is a_2, so that the period of the layer is $a = a_1 + a_2$. For simplicity, a_1/a will be referred to as the aspect ratio of the 1-D periodic layer. The thickness of the 1-D periodic layers is b_1 and the separation between two neighboring ones is b_2. In general, we assume that between two neighboring layers, there is a relative position shift of the distance s in the lateral direction, so that we may investigate the effect of a large class of array patterns on the propagation characteristics of a 2-D periodic medium by adjusting the parameter s in our analysis. For example, we have a square array pattern for $s = 0$ and a triangular array pattern for $s = 0.5a$. Notice that for an arbitrary value of s, $b = b_1 + b_2$ is not necessary the period of the structure in the y-direction. Actually, the structure has a period $\sqrt{s^2 + b^2}$ along the direction at the angle $\theta = \sin^{-1}(s/b)$ from the y-axis; nevertheless, the ratio b_1/b will be referred to as the aspect ratio in the y-direction.

3. Mathematical Formulation

[8] Since the scattering of plane-wave by a stack of 1-D periodic layers has been well developed as a rigorous boundary-value problem [*Hwang and Peng*, 2002; *Peng*, 1989; *Peng et al.*, 1975; *Tamir et al.*, 1964; *Hessel and Oliner*, 1965; *Hall et al.*, 1988], the derivation of the input-output relation for a 1-D periodic layer is briefly outlined here, while more details are referred to the literature [*Peng et al.*, 1975]. Specifically, the results in the form of input impedance and transfer matrices will be used as the building block to analyze the plane-wave scattering by the stack of periodic layers.

3.1. Input-Output Relation of 1-D Periodic Layer

[9] The 1-D periodic layer is assumed to be vertically uniform and is characterized by a relative dielectric constant that is periodic along the x-direction, as:

$$\varepsilon(x) = \varepsilon(x + d), \tag{1}$$

where d is the period. Due to the spatial periodicity, a set of Fourier components or space harmonics is generated everywhere in the structure; the propagation constant of the nth space harmonic in the x- direction is given by:

$$k_{xn} = k_x + n\frac{2\pi}{d}, \text{for n} = \ldots, -2, -1, 0, 1, 2, \ldots, \tag{2}$$

where k_x is the fundamental wavenumber along x-direction. Based on Floquet's theorem, the general field solutions can be expressed as a superposition of the complete set of space harmonics. With respect to the z-direction, the tangential electric and magnetic field solutions in 1-D periodic medium can be written, for the TE mode, as [*Peng et al.*, 1975]:

$$E_y(x,z) = \sum_{n=-\infty}^{\infty}\sum_{m=-\infty}^{\infty} P_{mn}V_m(z)e^{-jk_{xn}x} \tag{3a}$$

$$H_x(x,z) = -\sum_{n=-\infty}^{\infty}\sum_{m=-\infty}^{\infty} Q_{mn}I_m(z)e^{-jk_{xn}x} \tag{3b}$$

with the shorthand notations:

$$V_m(z) = e^{-j\mathbf{k}_{zm}z}c_m + e^{j\mathbf{k}_{zm}z}d_m \tag{4a}$$

$$I_m(z) = Y_m\left[e^{-j\mathbf{k}_{zm}z}c_m - e^{j\mathbf{k}_{zm}z}d_m\right], \tag{4b}$$

where k_{zm} is the propagation constant along z-direction of the mth mode and is determined from the dispersion relation of the periodic medium for a given k_{xm}, the propagation constant of the mth space harmonic as defined in equation (1). Once k_{zm} is obtained, the Fourier amplitudes, P_{mn} and Q_{mn} can then be determined in a straightforward manner. c_m and d_m are, respectively, the amplitudes of the forward and backward propagating waves of the mth mode in the 1-D periodic layer, and Y_m is the corresponding wave admittance.

[10] The field solutions in a uniform medium can be easily written as a superposition of all space harmonics, each propagating independently as a plane wave. By imposing the continuity of tangential field components across the interfaces between the periodic and uniform layers, we can obtain the input-output relations of the periodic layer. The detailed mathematical derivations can be found in *Hwang and Peng* [2002]; the most important results are the input impedance and the transfer matrices that are given, respectively, as:

$$\mathbf{Z}_{in} = \mathbf{Q}(\mathbf{I} + \mathbf{\Gamma}_{in})(\mathbf{I} - \mathbf{\Gamma}_{in})^{-1}\mathbf{P}^{-1} \tag{5a}$$

$$\mathbf{T} = \mathbf{Q}[\mathbf{I} + \mathbf{\Gamma}_{out}]\exp(-j\mathbf{k}_z d)(\mathbf{I} + \mathbf{\Gamma}_t)^{-1}\mathbf{Q}^{-1} \tag{5b}$$

with the shorthand notations:

$$\mathbf{\Gamma}_t = e^{-jk_z t}\mathbf{\Gamma}_{out}e^{-jk_z t} \tag{5c}$$

$$\mathbf{\Gamma}_{out} = (\mathbf{Z}_{out}\mathbf{P} + \mathbf{Q})^{-1}(\mathbf{Z}_{out}\mathbf{P} - \mathbf{Q}), \tag{5d}$$

where t is the thickness of the 1-D periodic layer, $\boldsymbol{Z}_{out}$ and $\boldsymbol{Z}_{in}$ are the output and input impedance matrices looking downward from the lower- and upper- surfaces of such 1-D periodic layer, respectively. It is noted that the uniform layer can be regarded as the limiting case of

1-D periodic layer with vanishing periodic variation. Thus, the input-output relation of uniform layer will be simply a diagonal matrix and can be derived without difficulty.

3.2. Scattering Characteristics of a Stack of 1-D Periodic Layers

[11] With the input-output relation and transfer matrix for a single periodic layer described above, we may employ successively, from the bottom to the top layer, the input-output relation of a unit cell that consists of a 1-D periodic layer in junction with a uniform one. Thus we can obtain the input impedance matrix looking downward from the top surface of the structure, Z_{dn}, that is, the relationship between the tangential electric and magnetic field vectors at the reference plane z = 0:

$$\underline{E}_t(0) = \mathbf{Z}_{dn}\underline{H}_t(0), \tag{6}$$

where $\underline{\mathrm{E}}_\mathrm{t}$ and $\underline{\mathrm{H}}_\mathrm{t}$ are infinite column vectors whose entries consist of the amplitudes of the tangential electric and magnetic fields in the incident region, such as air. In terms of the superposition of the incident and reflected waves, these column vectors may be written in the following form:

$$\underline{E}_t(0) = \mathbf{Z}_a(\underline{a} + \underline{b}) \tag{7a}$$

$$\underline{H}_t(0) = \underline{a} - \underline{b}, \tag{7b}$$

where the vector $\underline{a}$ and $\underline{b}$ represent the amplitudes of incident and reflected plane waves, respectively. The boundary condition in equation (6) on the tangential field components on the input surface at z = 0 leads to the following vector relation:

$$\underline{b} = \mathbf{\Gamma}\underline{a} \tag{8a}$$

$$\mathbf{\Gamma} = (\mathbf{Z}_a + \mathbf{Z}_{dn})^{-1}(\mathbf{Z}_{dn} - \mathbf{Z}_a), \tag{8b}$$

where Γ is the reflection matrix of the stack of periodic layers. Thus, the reflected amplitudes of all the space harmonics are now completely determined. We then obtain the tangential electric and magnetic field over the input surface by equation (7a). Furthermore, we can successively employ the transfer matrix of a unit cell, equation (5d), from the top to bottom layer to obtain the electric and magnetic fields everywhere within the structure under consideration.

3.3. Guiding Characteristics of the Stacks of 1-D Periodic Layers

[12] In the absence of any incident wave, $\underline{a} = 0$, and the existence of nontrivial solutions requires the condition:

$$\det(\mathbf{Z}_a + \mathbf{Z}_{dn}) = 0 \tag{9}$$

which is known as the transverse resonance condition, which defines the dispersion relation of the waveguide. Such a determinantal equation of infinite order must be truncated to a finite order for numerical analysis. We have implemented a computer code on the basis of the exact formulation described above to determine the dispersion root of the waveguide. Extensive results are obtained systematically for various structural parameters, in order to identify the wave propagation phenomena and their physical implications.

4. Numerical Results and Discussions

[13] Based on the exact formulation described in the preceding section, we are now in a position to carry out both qualitative and quantitative analyses of guiding characteristics in such a class of waveguides. First, we invoke the concept of parallel-plate waveguide to model the waves propagation inside the defect region. This allows us to identify in an easy manner various physical effects associated with the structure in hand and this will be particularly useful for practical considerations. Second, with the truncation of the infinite system of equations for the Fourier amplitude to a finite order, the numerical accuracy is carefully studied. It is noted that in the case of TM mode, considerable improvement on the convergence rate can be achieved by reformulating the eigenvalue problems [*Lalanne and Morris*, 1996; *Li*, 1996; *Ho et al.*, 1990; *Shen and He*, 2002]. After the numerical accuracy is assured, extensive numerical data are obtained to identify systematically important physical processes associated with the structure under consideration and to explore promising applications.

[14] The characteristic solutions of the class of 2-D periodic dielectric array certainly depend on the composition of the structure. Throughout this work, we shall consider the case where the relative dielectric constants of dielectric rod and surrounding medium are 11.4 and 1.0, with the aspect ratio along x and y directions to be 0.4 and 0.6, respectively. By a proper choice of the parameters a_1, a_2, b_1, b_2 and s, we can generate any array pattern. For example, we may have a triangular pattern for $s = 0.5a$, and a square pattern with $a_1 = a_2 = b_1 = b_2$ and the lateral shift $s = 0$. Specific examples are given below.

4.1. Contour of Constant Reflection Coefficient

[15] To investigate the reflection of a plane wave by a 2-D periodic dielectric array, contours of constant reflection coefficient are plotted against the frequency and the incident angle. These contours provide a simple and useful procedure for the design of a waveguide for a desired number of propagating modes.

[16] Figure 2 shows the contour of constant reflection coefficient for a finite stack of 1-D periodic layers. The

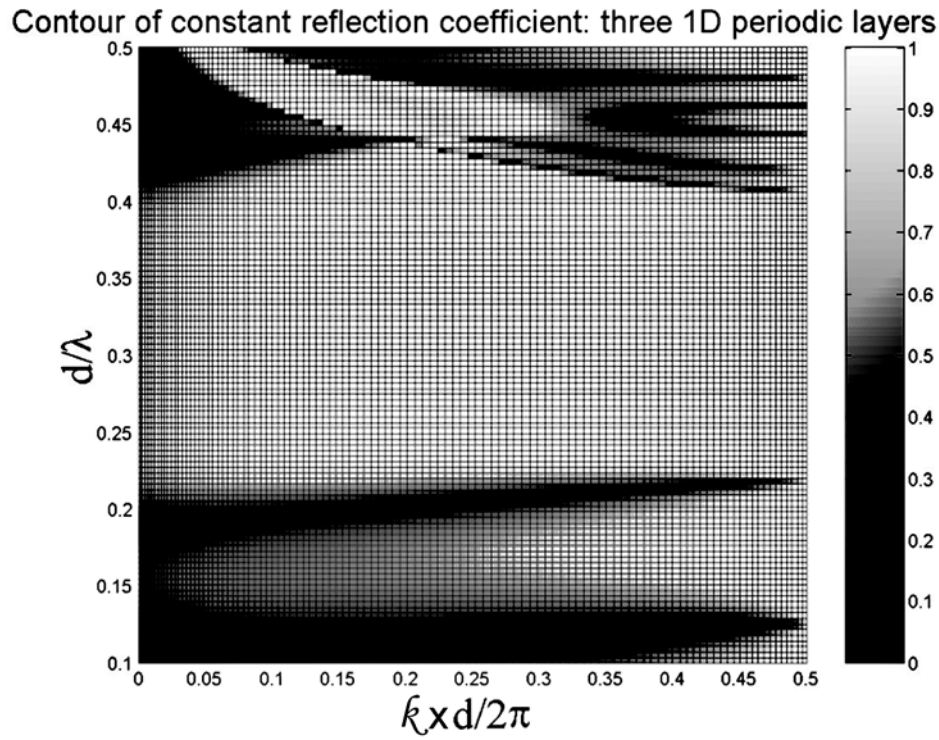

Figure 2. Contour of constant reflection coefficient for the stacks of 1-D periodic layer, where the number of stack is three.

horizontal axis represents the normalized phase constant along the x-direction, $k_x d/2\pi$, and the vertical axis shows the normalized frequency, d/λ. The reflectivity is plotted in gray-scale color map according to the level specified by the color bar on the right-hand side of the figure. The region drawn in bright color shows that of total reflection, that is, a reflection coefficient that is very close to unity. For example, the band where the normalized frequency (d/λ) is between 0.30 and 0.35 and the normalized phase constant ranges from 0 to 0.5 corresponds to the region of total reflection. Here, we may utilize the characteristics of total reflection in such a region for the design of waveguide walls, so that total internal reflections may be achieved with the wave bouncing back and forth between the two walls and its energy guided along this channel, as in the case of parallel-plate waveguide.

4.2. Dispersion Characteristics of Waveguide

[17] Before embarking on an elaborate numerical analysis, it is instructive to consider first the approximation of the dispersion relation by that of a corresponding ideal parallel-plate waveguide. The dispersion relation of a parallel-plate waveguide with a distance h between to metal plates can be expressed explicitly as:

$$\left(\frac{k_x d}{2\pi}\right)^2 + \left(\frac{nd}{2h}\right)^2 = \left(\frac{d}{\lambda}\right)^2 \varepsilon_a, \tag{10}$$

where d is the period of 1-D periodic layer along the x-direction, n is the mode index of the parallel-plate waveguide. Graphically, such a simple expression can be plotted into curve in the form of the Brillouin diagram, and the results are shown in dash line in Figure 3a. The above equation determines a parabolic curve with the normalized cutoff frequency located at $d/\lambda = d/2h$, for the lowest order mode of parallel-plate waveguide with either TE or TM polarization. Intuitively, we would expect a defect waveguide to behave in a similar way as a corresponding parallel-plate waveguide, if the total reflections from the waveguide walls are achieved. In what follows, we shall demonstrate that a parallel-plate waveguide can indeed provide useful initial data for the design of defect waveguides. As an example, in view of the contour map as shown in Figure 2, we may choose the cutoff condition of the "reference" parallel-plate wave at the value: $d/2h = 0.3$ so that its dispersion curve falls within the region of strong reflection of the stack of

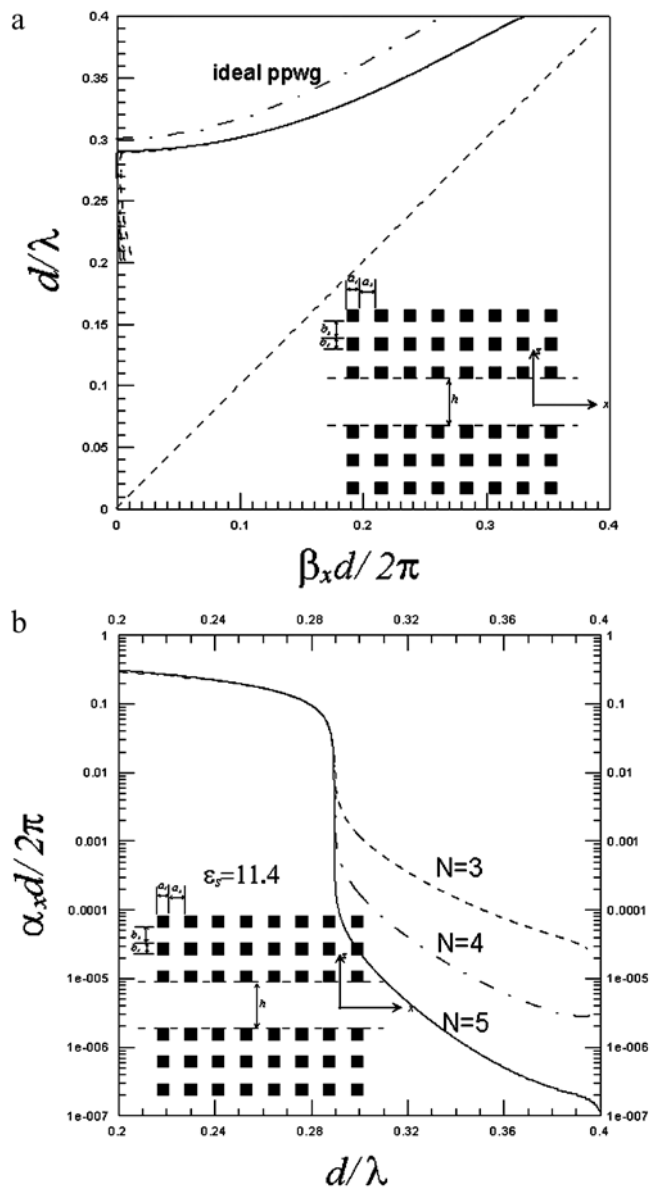

Figure 3. (a) Variation of the phase constant versus normalized frequency for different number of 1-D periodic layers; (b) variation of the attenuation constant versus normalized frequency for different number of 1-D periodic layers.

2-D periodic structure, as shown with a dash-dot line in (Figure 3a).

[18] Based on the exact dispersion relation in (10), we have carried out a systematically evaluation of the guiding characteristics of the waveguide walls with square pattern, and the results are likewise displayed in the form of Brillouin diagram in Figures 3a and 3b for real and imaginary parts of k_x, respectively. It is noted that the long-dash line is the boundary of the bound-wave region. The dispersion curves on the left-hand side of bound-wave boundary represent fast waves ($\beta_x \leq k_o$), while the those on the other side are slow waves ($\beta_x \geq k_o$). From Figure 3a we observe that the variation of phase constant for such a waveguide follows closely that of the corresponding parallel-plate waveguide, as expected. It is noted that in Figure 3a we have designed three cases of defect waveguide having three, four and five 1-D periodic layers as their waveguide walls, respectively. From this

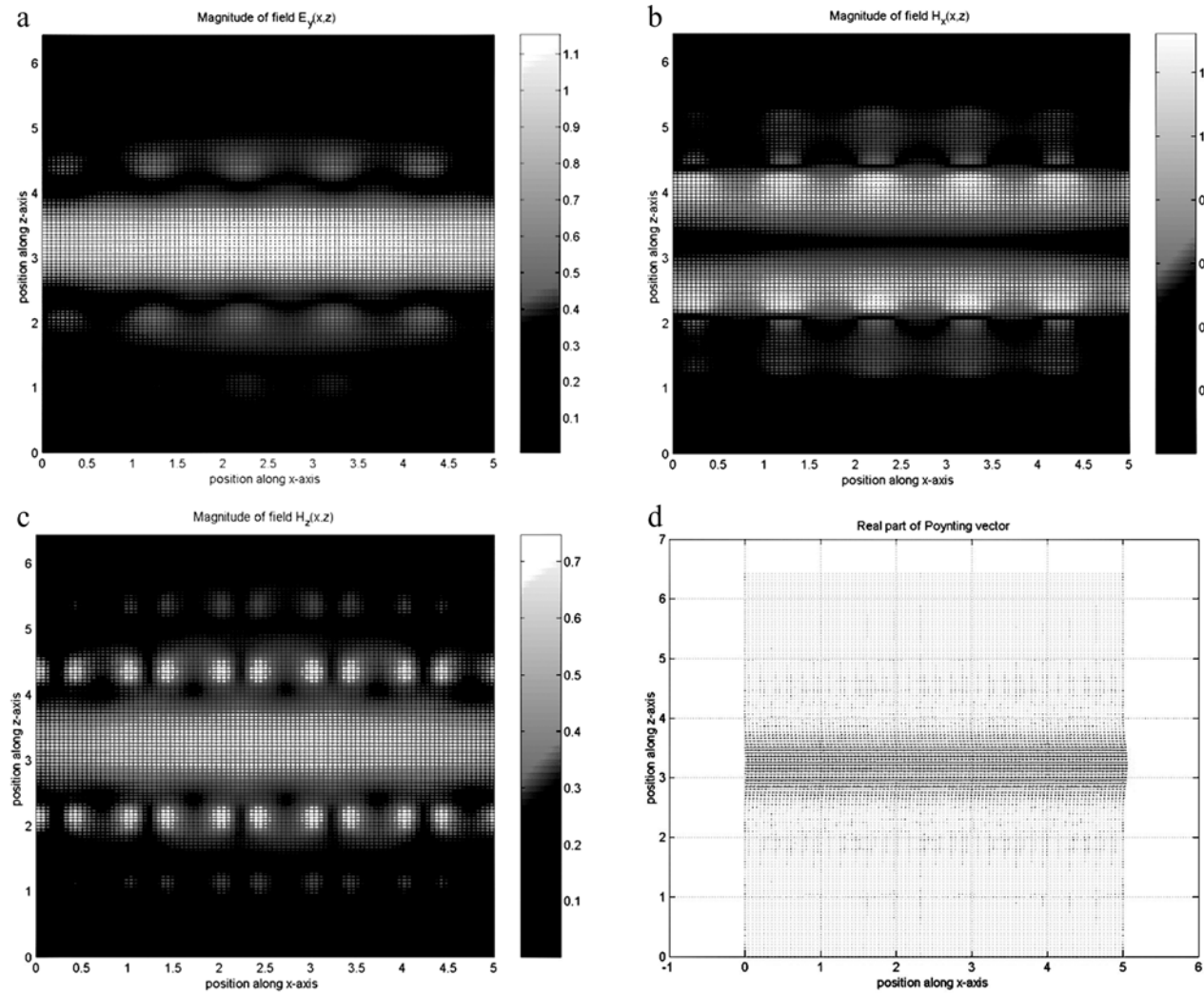

Figure 4. Distribution of electric and magnetic field components within the waveguide with 2-D periodic walls (guiding analysis), which is arranged in square pattern: (a) $E_y(x, z)$, (b) $H_x(x, z)$, and (c) H_z (x, z); (d) distribution of Poynting vector.

figure we observe that the increase of the number of 1-D periodic layers has a negligible effect on the phase constant, but it reduces appreciably the attenuation due to the leakage of energy through the 1-D periodic layers of finite number, as depicted in Figure 3b.

4.3. Field Contour Plot

[19] To substantiate the guiding characteristics of waveguide modes in such waveguide, we plot the contour of electric and magnetic field components for easy understanding of the physical picture of the wave-guiding phenomenon. First, we arbitrarily choose one point ($d/2h = 0.3175$) on the dispersion curve to plot the field distribution, as shown in Figures 4a, 4b, and 4c, respectively, for E_y, H_x and H_z over the waveguide with square pattern of walls. It is noted that these fields are plotted with the normalization of the eigenvector, corresponding to the dispersion root (eigenvalue) as determined from equation (9), to unity. Referring to the color bar attached, Figure 4a indicates that the electric field is concentrated in the waveguide region and exhibits the localization of power within it. Away from this region, the fields decay exponentially in the transverse direction.

4.4. Distribution of Poynting Vector

[20] In addition to the field contour as shown previously, Poynting vector can also provide us considerable information about the power flow in waveguide. We setup a grid with a large number of points in the structure

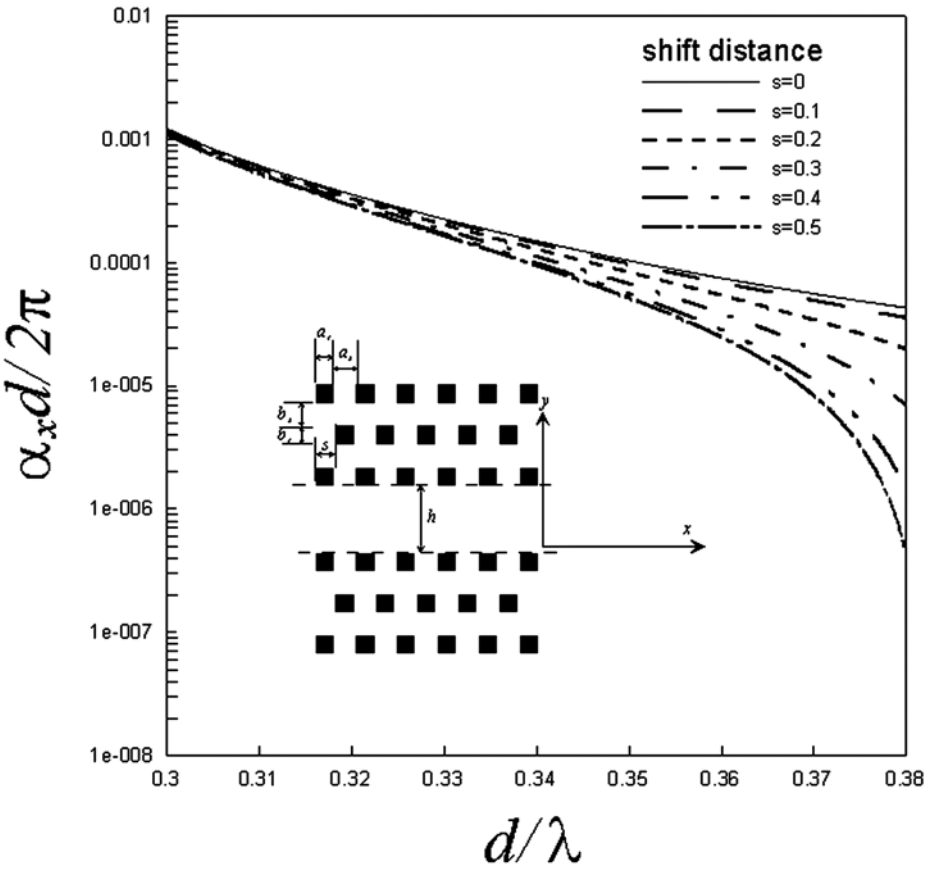

Figure 5. Variation of the attenuation constant versus normalized frequency for various lattice patterns.

and determine the Poynting vector at each of those grid points. By the normalization of the amplitude of the incident plane wave to unity, the resulting pattern is shown in Figure 4d with the same parameters as those in Figures 4a–4c. As is well known, the real part of Poynting vector represents the strength and direction of power flow. In Figure 4d the distribution of the Poynting vectors is almost uniform in the central region and is flowing along the axial direction. On the other hand, the Poynting vectors away from the waveguide are rather small; thus, the power leakage is negligible, consistent with the fact that the attenuation constant is quit small.

4.5. Influence of the Lattice Pattern on the Propagation Constant of the Localized Mode

[21] In addition to the square pattern, we have also investigated the dispersion relation for various patterns with different lateral shift distance s ranging from zero to a half of the period along x direction. Though not shown, we have found that the variations of the phase constant do not change appreciably. In contrast, as shown in Figure 5, the attenuation constants among them vary significantly. To the extent of our calculations, the attenuation constants of square and triangular pattern yield, respectively, lower and upper bounds of all the patterns. From these results we may conclude that the triangular pattern yields the strongest stop-band behavior. This provides a general guideline for the selection of array pattern for a specific purpose, tightly bound or otherwise.

4.6. Strong Coupling Between Incident Plane Wave and Localized Modes in Defect Waveguide

[22] We have carried out extensive numerical experiments with various structure and incident parameters; however, only a few representative sets are selected here to illustrate the interesting phenomena that may take place in the presence of 2-D periodic structure. Figure 6a shows the reflection intensity of the space harmonic $n = 0$ versus the wavelength of the plane wave for various incident angles. It is important to observe that there exists a sharp

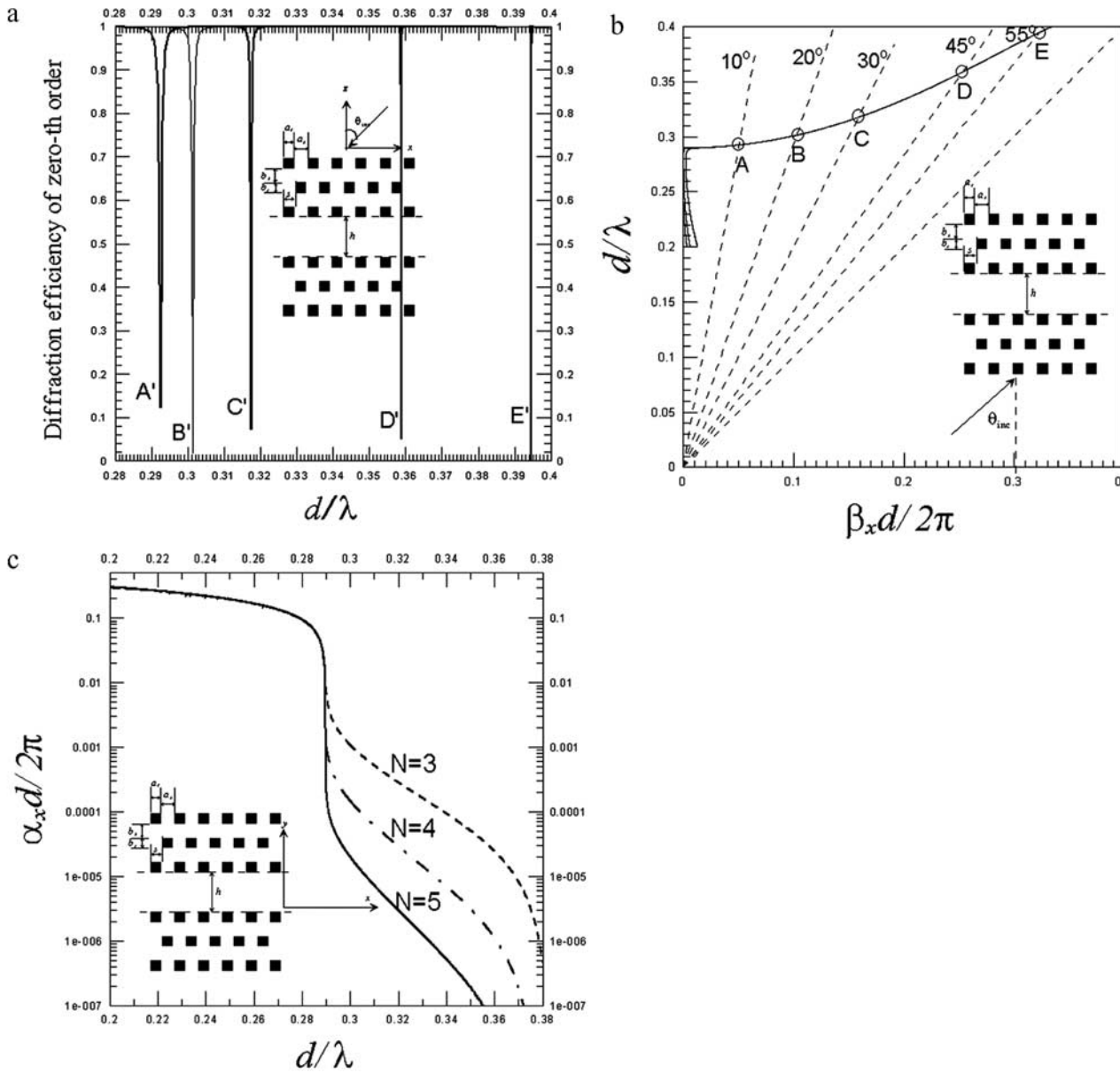

Figure 6. (a) Variation of the reflection intensity versus normalized frequency for various incident angles; the number of 1-D periodic layer is three and is arranged in triangular pattern; variation of the phase constant (b) and attenuation constant (c) versus normalized frequency for different number of 1-D periodic layers arranged in triangular pattern.

variation along each curve, as marked by the characters from A's to E's in Figures 6a and 6b.

[23] To explain these unusual behaviors of reflection characteristics, we recall the dispersion curve of waveguide with 2-D periodic walls of triangular pattern. Referring to the inset in Figure 6b, a plane wave of TE polarization is incident on such a waveguide at an angle θ_{inc} with respect to the z-axis. The phase constant k_x along the x-direction is given as:

$$k_x = k_o \sin\theta_{inc}, \tag{11}$$

where k_o is the free-space wavenumber. For a given incident angle θ_{inc}, the relationship between $k_x d/2\pi$ and

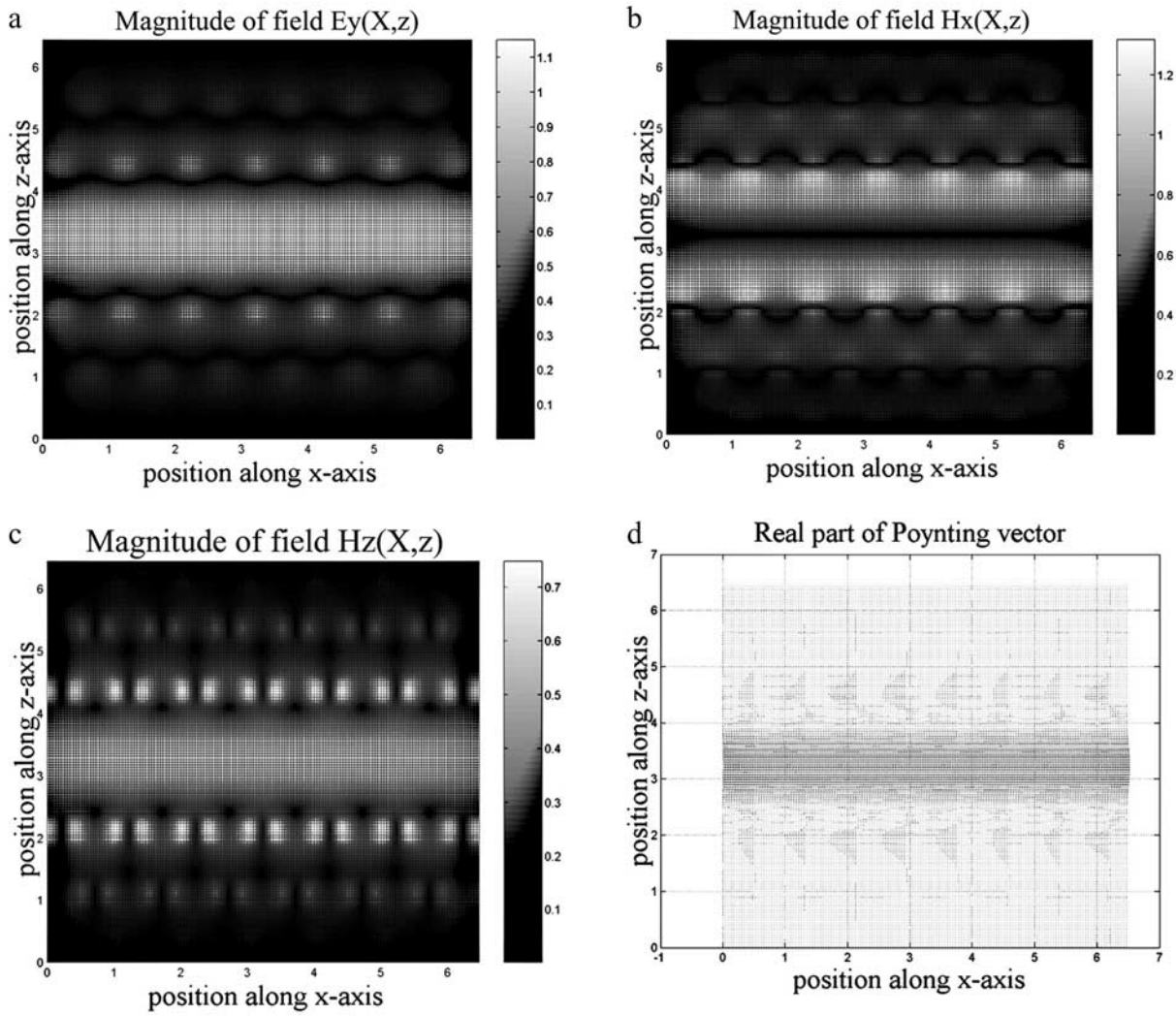

Figure 7. Distribution of electric and magnetic field components within the waveguide with 2-D periodic walls (scattering analysis), which is arranged in triangular pattern: (a) $E_y(x, z)$, (b) $H_x(x, z)$, and (c) $H_z(x, z)$; (d) distribution of Poynting vector.

$k_o d/2\pi$ can be represented as a straight line passing through the origin with the slope $1/\sin\theta_{inc}$. Here, we plot the straight line for various angles together with the Brillouin diagram in Figure 6b. Here, the intersection points between incident plane wave and waveguide mode are circled and labeled in alphabetical order for various incident angles. At each of the intersection points, the real part of the wavenumber along the x direction of waveguide mode is the same as that of incident plane wave, and this is known as the phase-matching condition for maximum coupling. Over the frequency range covering all intersection points, we had calculated the reflected power under the same incident conditions, as shown in Figure 6a.

[24] Explicitly, we observe that the sharp decreases in the bandwidth occur at different frequencies as marked by the characters A′, B′, C′, D′ and E′, respectively. Comparing to Figure 6b, the position of rapid variation corresponds to the intersection points A, B, C, D and E, respectively. It is interesting to note that these intersection points have very small attenuation constant for the waveguide, as shown in Figure 6c; thus, good phase-matching conditions occurs at these points, and a strong coupling takes place between the incident plane wave

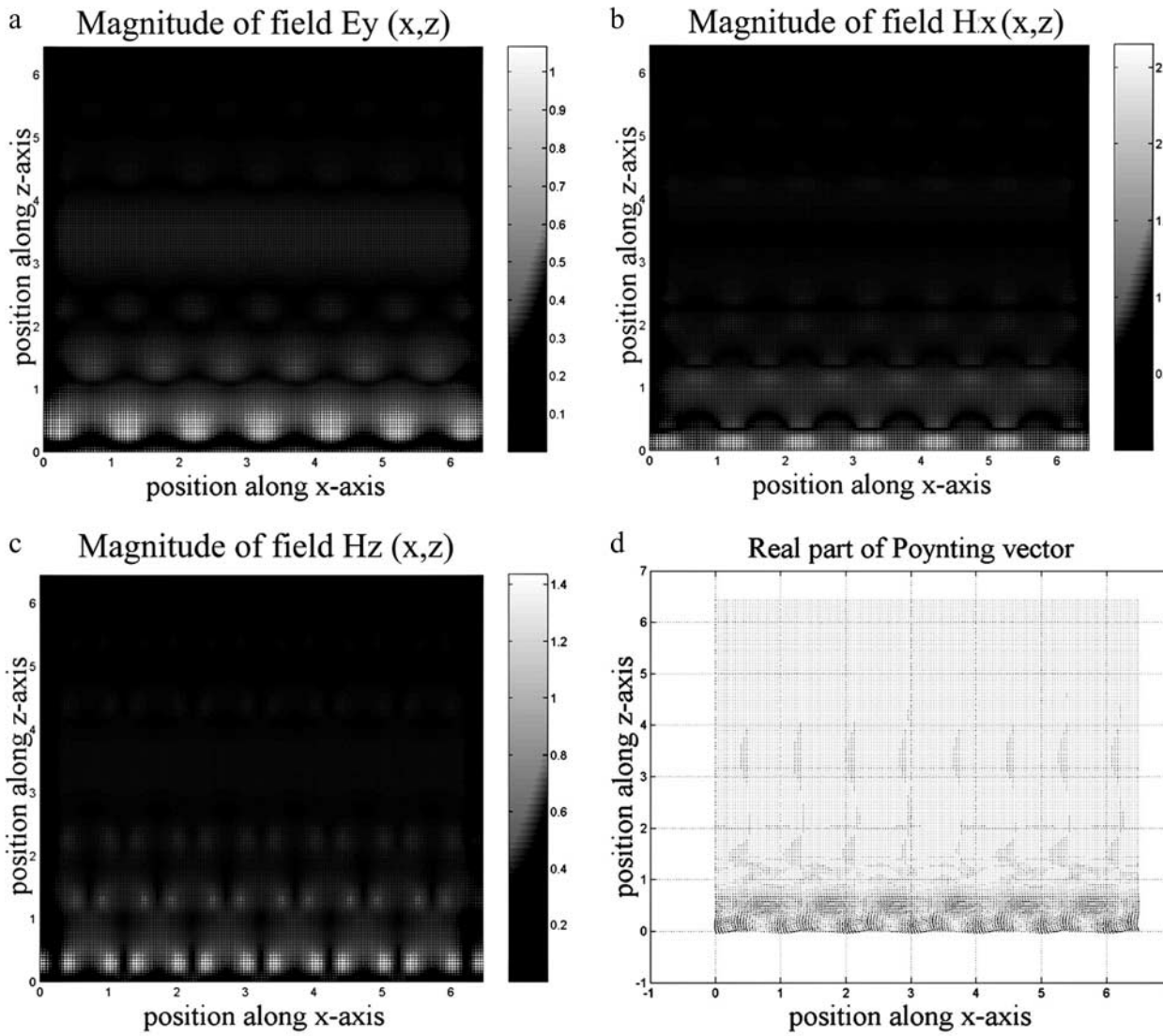

Figure 8. Distribution of electric and magnetic field components within the waveguide with 2-D periodic walls (scattering analysis), which is arranged in triangular pattern: (a) $E_y(x, z)$, (b) $H_x(x, z)$, and (c) $H_z(x, z)$; (d) distribution of Poynting vector.

and a waveguide mode. In particular, the two cases C and D have very narrow bandwidths, because these are high-Q operation with the attenuation constant of waveguide nearly equal to zero.

[25] To understand the coupling of energy under the phase-matching condition, we also plot the contour for the electric and magnetic field components, as we have done in the previous example. Here, the incident angle is designated as 30° and the normalized frequency is $d/\lambda = 0.317$, which is located at the intersection point C. It is interesting to note that the field pattern shown in Figures 7a to 7d is identical to that shown in Figure 4. It is evident that under the phase-matching condition, the energy of the incident plane wave is converted into that of the waveguide.

[26] In contrast to the phase-matching condition between the incident plane wave and a waveguide mode, we choose a point away from the intersection point, that is, the incident angle is $\theta_{inc} = 30°$ and the normalized frequency is $d/\lambda = 0.35$. Since this operation point is not at the phase-matching condition, the incident power can't be coupled into the waveguide and must be reflected

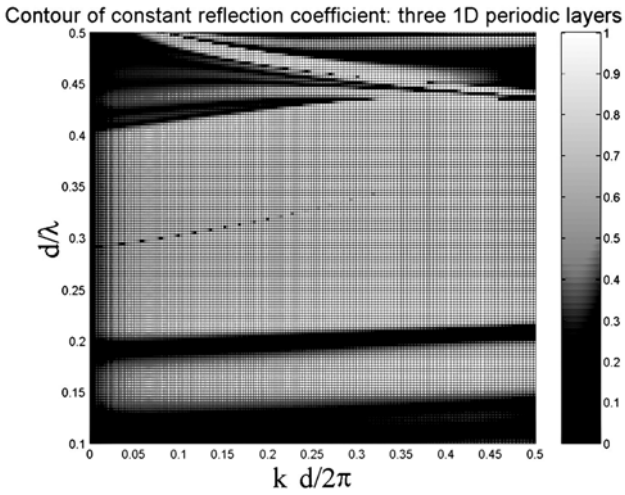

Figure 9. Contour plot of constant reflection coefficient within the waveguide with 2-D periodic walls, which is arranged in square pattern; scattering analysis.

back into the free-space under the stop-band condition. The contour of field components and distribution of Poynting vector are shown in Figures 8a to 8d, which indicate that the incident plane wave is indeed reflected by the structure and can hardly penetrate into the structure.

[27] Figure 9 shows the contour of constant reflection coefficient for the waveguide with triangular pattern of waveguide walls. In this example, we plot the contour map versus both normalized frequency and phase constant along the *x*-direction. It is interesting to note that there exists a parabolic curve with low reflectivity, which is the same that as shown in Figure 6b. This can now be explained on the basis of the phase-matching condition. Therefore, as long as the attenuation constant of waveguide mode is not too large, the phase constant of waveguide mode can be predicted by the phase-matching condition for the scattering analysis or vice versa.

5. Conclusions

[28] We have employed the rigorous method of mode matching to treat the problem of scattering and guiding characteristics of waveguides with 2-D periodic walls of finite thickness. We analyze first the scattering of plane waves by a 2-D periodic dielectric array to identify its stopband behavior. The results are then utilized for the study of guiding characteristics of waveguide composed of 2-D periodic arrays as its side walls. In particular, the strong coupling of incident plane wave into a waveguide mode has been investigated and was utilized to predict the guiding characteristic of the waveguide. Extensive numerical results have been carried out to investigate the phenomena of energy leakage for various numbers of layers in a stack and also for different array patterns. We have demonstrated that an ideal parallel-plate waveguide can provide useful initial data for the design of defect waveguides.

[29] **Acknowledgments.** This research work was supported jointly by the Ministry of Education and Economic Affairs (Phtotonics System on Chip) under the contact numbers 89-E-FA06-2-4 and 91-EC-17-A-07-S1-0011.

References

Gauthier, G. P., A. Courtay, and G. M. Rebeiz, Microstrip antennas on synthesized low dielectric-constant substrates, *IEEE Trans. Antennas Propag.*, *45*, 1310–1314, 1997.

Hall, R. C., R. Mittra, and K. M. Mitzner, Analysis of multilayered periodic structures using generalized scattering matrix theory, *IEEE Trans. Antennas Propag.*, *36*, 511–517, 1988.

Hessel, A., and A. A. Oliner, A new theory of Wood's anomalies on optical gratings, *Appl. Opt.*, *4*, 1275–1297, 1965.

Ho, K. M., C. T. Chan, and C. M. Soukoulis, Existence of a photonic gap in periodic dielectric structures, *Phys. Rev. Lett.*, *65*, 3152–3155, 1990.

Hwang, R. B., and S. T. Peng, Guidance characteristics of two-dimensional periodic impedance surface, *IEEE Trans. Microwave Theory Tech.*, *47*, 2503–2511, 1999a.

Hwang, R. B., and S. T. Peng, Guided waves on 2-D periodic structures and their relation to planar photonic band gap structures, *IEICE Trans. Electron.*, *E83-C*, 705–712, 1999b.

Hwang, R. B., and S. T. Peng, Properties of waveguides with periodic side walls of finite width, paper presented at Conference on Progress in Electromagnetic Research, Boston, Mass., 2002.

Joannopoulos, J. D., R. D. Meade, and J. N. Winn, *Photonic Crystal*: *Modeling the Flow of Light*, Princeton Univ. Press, Princeton, N. J., 1995.

Lalanne, P., and G. M. Morris, Highly improved convergence of the coupled-wave method for TM polarization, *J. Opt. Soc. Am. A.*, *13*, 779–784, 1996.

Larsen, R. P., and A. A. Oliner, A new class of low loss reactive wall waveguides, paper presented at G-MTT International Microwave Symposium Program and Digest, 1967.

Li, L., Use of Fourier series in the analysis of discontinuous periodic structures, *J. Opt. Soc. Am. A.*, *13*, 1870–1876, 1996.

Lubecke, V. M., K. Mizuno, and G. M. Rebeiz, Micromachining for terahertz applications, *IEEE Trans. Microwave Theory Tech.*, *46*, 821–831, 1998.

Maystre, D., Electromagnetic study of photonic band gaps, *Pure Appl. Opt.*, *3*, 975–993, 1994.

Mekis, A., S. Fan, and J. D. Joannopoulos, Absorbing boundary conditions for FDTD simulations of photonic crystal wave-

guides, *IEEE Microwave Guided Wave Lett.*, *9*, 502–504, 1999.

Noponen, E., and J. Turunen, Eigenmode method for electromagnetic synthesis of diffractive elements with three-dimensional profiles, *J. Opt. Soc. Am. A*, *11*, 2494–2502, 1994.

Papapolymerou, R., F. Drayton, and L. P. B. Katechi, Micromachined patch antennas, *IEEE Trans. Antennas Propag.*, *46*, 275–283, 1998.

Peng, S. T., Rigorous formulation of scattering and guidance by dielectric grating waveguides: General case of oblique incidence, *J. Opt. Soc. Am.*, *6*, 869–883, 1989.

Peng, S. T., T. Tamir, and H. L. Bertoni, Theory of dielectric grating waveguides, *IEEE Trans. Microwave Theory Tech.*, *23*, 123–133, 1975.

Shen, L., and S. He, Analysis for the convergence problem of the plane-wave expansion method for photonic crystals, *J. Opt. Soc. Am. A.*, *19*, 1021–1024, 2002.

Shen, L., S. He, and S. Xiao, Large absolute band gaps in two-dimensional photonic crystals formed by large dielectric pixels, *Phys. Rev. B*, *66*, 165,315–165,320, 2002.

Sievenpiper, D., L. Zhang, R. F. Jimenez Broas, N. G. Alexopolous, and E. Yablonovitch, High-impedance electromagnetic surface with a forbidden frequency band, *IEEE Trans. Microwave Theory Tech.*, *47*, 259–274, 1999.

Tamir, T., H. C. Wang, and A. A. Oliner, Wave propagation in sinusoidally stratified dielectric media, *IEEE Trans. Microwave Theory Tech.*, *12*, 323–330, 1964.

Vardaxoglou, J. C., A. Hossainzadeh, and A. Stylianou, Scattering from two-layer FSS with dissimilar lattice geometries, *Microwaves Antennas Propag. IEE Proc. H*, *140*, 59–61, 1993.

Yang, D. H. Y., Finite difference analysis of 2-D photonic crystals, *IEEE Trans. Microwave Theory Tech.*, *44*, 2688–2695, 1996.

Yang, F.-R., K.-P. Ma, Y. Qian, and T. Itoh, A novel TEM waveguide using uniplanar compact photonic-bandgap (UC-PBG) structure, *IEEE Trans. Microwave Theory Tech.*, *47*, 2092–2098, 1999.

R. B. Hwang, Graduate Institute of Communication Engineering, National Chi Nan University, Puli, Nantou, 545 Taiwan. (rbhwang@ncnu.edu.tw)

S. T. Peng, Microelectronics and Information Systems Research Center, National Chiao-Tung University, Hsinchu, 300 Taiwan.